

Double Layer Forces over Large Potential Ranges as Measured in an Electrochemical Surface Forces Apparatus

Joëlle Fréchet and T. Kyle Vanderlick*

Department of Chemical Engineering, Princeton University, Princeton, New Jersey 08544

Received July 16, 2001. In Final Form: September 6, 2001

Electrodes specifically designed for use in the surface forces apparatus (SFA) were employed to study forces between mica and polycrystalline gold under potential control. This control was achieved by soldering a wire to the gold surface and modifying the chamber of the SFA into a three-electrode cell configuration. The interactions measured were a strong function of the applied electrode potential, being more repulsive as the gold potential was moved toward more negative potentials. Independent force measurements between mica surfaces were done to determine the mica surface potential. The experimental results were compared to Derjaguin–Landau–Verwey–Overbeek (DLVO) predictions of the forces between dissimilar charged surfaces. The long range forces correspond well to DLVO predictions, including evidence of saturation in forces at high applied potentials; forces deviate from theory at short range.

Introduction

All surface phenomena are, to some degree, dependent on surface potential. Electrochemical synthesis, adsorption, and adhesion are key examples. The ability to vary the surface potential of a substrate, as is possible in an electrochemical cell, provides a powerful handle for controlling chemical reactions and, more generally, for tuning surface properties. In the case of adsorption, changing the surface potential can change the orientation of an adsorbate or even induce complete desorption.¹ Adsorbed surfactants have also been shown to make potential dependent patterns on gold² and DNA helices align as an electric field is applied.³

One of the most significant potential dependent events is the establishment of the electrical double layer in solution surrounding a charged surface. This inhomogeneous spatial distribution of charge carriers arises from the need to maintain charge neutrality. Because of the limited supply of ions in solution, the double layer can extend tens of nanometers beyond the electrode surface, a manifestation of the nonlocal effects of surface potential. Hence, when two charged surfaces approach each other, the overlap of their double layers gives rise to long range forces; such interactions are central to many phenomena such as colloidal stability and clay swelling.⁴ The study of double layer structure is also fundamental to a variety of disciplines ranging from electrochemistry⁵ to biology.⁶

The development of techniques for direct force measurements has played a key role in the quest to understand the nature of the electrical double layer. One of the most prominent is the surface force apparatus (SFA),^{7,8} which

came on the scene over 30 years ago. Here, the force between opposing surfaces is measured via the deflection of a leaf spring on which one of the surfaces is mounted, and the surface separation is deduced independently using multiple beam interferometry (MBI).⁹ The pioneering work of Israelachvili and Pashley has provided one of the most definitive sets of double layer force measurements to date.^{10–14} Notably, however, the SFA has been utilized to only a fraction of its capacity as the apparatus has been used mainly to study forces acting between two mica surfaces. Few studies have employed the SFA to examine surface forces associated with having a metal surface in aqueous solution.^{15–18} In these experiments, however, the metal surface was not set in an electrochemical environment and there was no control of surface potential.

The advent of the atomic force microscope (AFM),¹⁹ modified to measure forces in liquid,^{20,21} has stimulated a host of studies on the structure and behavior of various electrochemical interfaces.^{22–32} For example, Ishino et al.²² controlled the electrical potential of a gold-coated canti-

* To whom correspondence should be addressed. Phone, (609)-258-4891; fax, (609)258-0211; e-mail, vandertk@princeton.edu.

(1) Stolberg, L.; Richer, J.; Lipkowski, J.; Irish, D. E. *J. Electroanal. Chem.* **1986**, *207*, 213–234.

(2) Burgess, I.; Jeffrey, C. A.; Cai, X.; Szymanski, G.; Galus, Z.; Lipkowski, J. *Langmuir* **1999**, *15*, 2607–2616.

(3) Kelley, S. O.; Barton, J. K.; Jackson, N. M.; McPherson, L. D.; Potter, A. B.; Spain, E. M.; Allen, M. J.; Hill, M. G. *Langmuir* **1998**, *14*, 6781–6784.

(4) Hunter, R. J. *Foundations of Colloid Science*; Oxford University Press: New York, 1986; Vol. 1.

(5) Bard, A. J. *J. Phys. Chem.* **1993**, *97*, 7147–7173.

(6) Israelachvili, J. N. *Intermolecular and Surface Forces with Applications to Colloidal and Biological Systems*; Academic Press: London, 1985.

(7) Tabor, D.; Winterton, R. H. S. *Proc. R. Soc. London, Ser. A* **1969**, *312*, 435–450.

(8) Israelachvili, J. N.; Adams, G. E. *J. Chem. Soc., Faraday Trans. 1* **1978**, *74*, 975–1001.

(9) Tolansky, S. *Multiple-Beam Interferometry of Surfaces and Films*; Oxford University Press: London, 1948.

(10) Pashley, R. M. *J. Colloid Interface Sci.* **1981**, *80*, 153–162.

(11) Pashley, R. M. *J. Colloid Interface Sci.* **1981**, *83*, 531–546.

(12) Pashley, R. M. *Adv. Colloid Interface Sci.* **1982**, *16*, 57–62.

(13) Pashley, R. M.; Israelachvili, J. N. *J. Colloid Interface Sci.* **1984**, *97*, 446–455.

(14) Pashley, R. M.; Quirk, J. P. *Colloids Surf.* **1984**, *9*, 1–17.

(15) Smith, C. P.; Maeda, M.; Atanasoka, L.; White, H. S.; McCure, D. J. *J. Phys. Chem.* **1988**, *92*, 199–205.

(16) Coakley, C. J.; Tabor, D. *J. Phys. D: Appl. Phys.* **1978**, *11*, L77–L82.

(17) Parker, J. L.; Cristenson, H. K. *J. Chem. Phys.* **1988**, *12*, 8013–8014.

(18) Ederth, T.; Claesson, P.; Liedberg, B. *Langmuir* **1998**, *14*, 4782–4789.

(19) Binnig, G.; Quate, C. F.; Gerber, C. *Phys. Rev. Lett.* **1986**, *56*, 930–933.

(20) Ducker, W.; Senden, T. J.; Pashley, R. M. *Nature* **1991**, *353*, 239–241.

(21) Ducker, W. A.; Senden, T. *Langmuir* **1992**, *8*, 1831–1836.

(22) Ishino, T.; Heida, H.; Tanaka, K.; Gemma, N. *J. Appl. Phys.* **1994**, *33*, 1552–1554.

(23) Hillier, A. C.; Kim, S.; Bard, A. J. *J. Phys. Chem. B* **1996**, *100*, 18808.

(24) Raiteri, R.; Grattarola, M.; Butt, H.-J. *J. Phys. Chem. B* **1996**, *100*, 16700–16705.

lever and measured forces between the cantilever and the glass substrates covered with different monolayers. Hillier et al.²³ varied the potential of a gold substrate and measured its interaction with a silica particle, showing that forces followed Derjaguin–Landau–Verwey–Overbeek (DLVO) theory; they also studied the relationship between the point of zero force and the point of zero charge. Raiteri et al.²⁴ applied electrical potential on a gold substrate and measured its interaction with a nonconducting silicon nitride tip. They investigated surfaces at high potentials and observed a very steep increase in forces over a small potential window. A similar effect was seen by Arai and Fujihira,²⁵ who controlled the potential of both interacting surfaces; however, their theoretical fits indicated values of surface potential higher than expected. Raiteri et al.²⁸ later also controlled the potential of both interacting surfaces with similar results.

The AFM and the SFA provide two complementary approaches to study surface interactions. For example, forces measured with the SFA are in mechanical equilibrium (static), given that time is allowed between each measurement for surface separation to stabilize. This is not the case for the AFM, where measurements are inherently dynamic since the deflection of the cantilever is monitored while the sample is mounted on an oscillating piezoelectric.³³ Length scales are another major difference between AFM and SFA measurements. When a colloidal sphere is attached to the AFM cantilever tip, the interacting area is on the order of $0.1 \mu\text{m}^2$. The radius of curvature of the cylindrical substrates used in the SFA is between 1 and 2 cm; when oriented in the prescribed crossed cylinder geometry, the interacting areas are on the order of $100 \mu\text{m}^2$.²⁴ It thus may be argued that the AFM is better suited to study events on a molecular scale while the SFA is better suited for probing phenomena associated with surfaces of a defined area and/or with nonidealized character (e.g., rough), as might be used in engineering applications. Perhaps the most striking difference between the two techniques is in how surface separation is determined. In the SFA, surface separation is independently measured via interferometry; moreover, the optical technique allows direct determination of the geometry of the interacting substrates (e.g., effective radius of curvature). In contrast, the separation in an AFM experiment is inferred from the forces observed. In particular, contact is usually associated with the onset of a regime of constant compliance. Such an assignment can be confounded, for example, by the presence of hard adsorbed films or molecular layers, ill-defined contacts such as those associated with rough surfaces, and dynamic changes in surface structure.

The technological need for a better understanding of the electrode/electrolyte interface serves as a strong incentive to further develop the SFA. This would, for example, allow the study of adhesion and tribological issues associated with microelectromechanical systems (MEMS).³⁴ The device would also be particularly useful

for investigating heterocoagulation and other colloidal phenomena such as electrodeposition. Such an advanced electrochemical surface forces apparatus (ESFA) could also be a powerful tool for investigating potential dependent adsorption phenomena. In addition to probing the changes in forces arising from different adsorption states, the exquisite sensitivity of the interferometry might be exploited to obtain information on the presence (and even orientation) of molecular adsorbates.

One approach in this regard is to use a mercury drop electrode as one of the interacting surfaces, as pioneered by Connor and Horn.³⁵ A key advantage of this approach is the availability of a clean and molecularly smooth electrode surface as provided by the mercury drop; however, a complication (although of interest in its own right) is the resultant deformation of this liquid substrate in response to forces of interaction. We have thus embarked on an alternative approach in which a solid substrate, in particular gold, functions as the electrode.

In this paper, we use a new technique for controlling surface potential in the SFA to probe double layer forces between a mica and a gold electrode. We observe a large potential range for surface forces as well as the onset of force saturation, which is expected at high potential. We compare our results with DLVO theory as well as with experimental studies of others using AFM.

The paper is organized as follows. We provide a Background section for describing the key points of DLVO theory in the context of fitting direct force measurements. We then devote a separate section to a description of our technique for electrode formation and its use in the ESFA. The remainder of the paper (Experimental Section followed by Results and Discussion) reports on our observations of double layer forces measured over large potential ranges as made possible with the new technique.

Background

The well-known DLVO^{36,37} theory of colloid stability predicts that the interaction energy (V_T) between colloid particles is a superposition of two independent interactions: van der Waals (V_{vdW}) and electrostatic (V_E). The forces measured between curved surfaces are related to the interaction energy per unit area through the Derjaguin³⁸ approximation.

The electrostatic interaction energy is caused by the overlap of the electrical double layers of the opposing surfaces. The resulting normal stress (T_{xx}) supported by the fluid confined between the surfaces is (for a 1:1 electrolyte)

$$T_{xx} = 2n_b kT \cosh(e\psi/kT) - \frac{\epsilon_r \epsilon_0}{2} \left(\frac{d\psi}{dx} \right)^2 \quad (1)$$

where the first term corresponds to an osmotic stress and the second is the so-called Maxwell stress, which is always attractive. ψ is the local potential (which varies with position, x , between the plates), n_b is the bulk concentration, ϵ_r is the dielectric constant, ϵ_0 is the permittivity of free space, e is the elementary charge, k is the Boltzmann constant, and T is temperature. The local osmotic stress and local Maxwell stress vary from point to point across the gap such that the total normal stress is constant. For

(25) Arai, T.; Fujihira, M. *J. Vac. Sci. Technol., B* **1996**, *14*, 1378–1382.

(26) Hu, K.; Bard, A. J. *Langmuir* **1997**, *13*, 5114–5119.

(27) Hu, K.; Bard, A. J. *Langmuir* **1997**, *13*, 5418–5425.

(28) Raiteri, R.; Preuss, M.; Grattarola, M.; Butt, H.-J. *Colloid Surf., A* **1998**, *136*, 191–197.

(29) Campbell, S. D.; Hiller, A. C. *Langmuir* **1999**, *15*, 891–899.

(30) Doppenschmidt, A.; Butt, H.-J. *Colloid Surf., A* **1999**, *149*, 145–150.

(31) Wang, J.; Bard, A. J. *J. Phys. Chem. B* **2001**, *105*, 5217–5222.

(32) Wang, J.; Bard, A. J. *J. Am. Chem. Soc.* **2001**, *123*, 498–499.

(33) Vinogradova, O. I.; Butt, H. J.; Yakubov, G. E.; Feuillebois, F. *Rev. Sci. Instrum.* **2001**, *72*, 2330–2339.

(34) Komvopoulos, K. *Wear* **1996**, *200*, 305–327.

(35) Connor, J. N.; Horn, R. G. *Langmuir*, in press.

(36) Derjaguin, B. V.; Landau, L. *Acta Physicochim URSS* **1941**, *14*, 633–662.

(37) Verwey, E. J. W.; Overbeek, J. T. *Theory of Stability of Lyophobic Colloids*; Elsevier: New York, 1948.

(38) Derjaguin, B. V. *Kolloid-Z.* **1934**, *69*, 155.

the case of symmetrical double layers, this normal stress is most easily evaluated at the gap midplane where the Maxwell stress is zero. The electrostatic interaction energy (V_E) is the work required to bring the plates from infinity to a given separation (D).

van der Waals interaction is always attractive and in the nonretarded case can be expressed as a function of separation (D) with a Hamaker (A_H) constant in the form

$$V_{\text{vdW}} = - (A_H/12\pi D^2) \quad (2)$$

Force predictions made using DLVO theory require as input the potential distribution, $\psi(x)$. On the basis of the Gouy–Chapman model,^{39,40} this distribution satisfies the nonlinear Poisson–Boltzmann equation

$$\frac{d^2\psi}{dx^2} = \frac{2en_b}{\epsilon_r\epsilon_0} \sinh\left(\frac{e\psi}{kT}\right) \quad (3)$$

The charging behavior of the surfaces as they approach sets the boundary conditions on the potential distribution. Two limiting cases are generally considered, constant charge density and constant potential. The constant charge situation yields an upper bound on the force, while constant potential establishes a lower bound. Other types of boundary conditions, such as charge regulation,^{41,42} may also be formulated.

Solving the Poisson–Boltzmann equation is a separate matter. Analytical solutions exist for the case of two surfaces at the same potential.^{4,6} Some analytical approximations have been developed for dissimilar surfaces.^{43,44} At low surface potentials (generally less than 25 mV), the linearized Poisson–Boltzmann equation is often used.⁴⁵ Of course, one can always solve the nonlinear Poisson–Boltzmann equation numerically (using, for example, Newton's method to converge on a solution). This approach eliminates the inaccuracies associated with approximations, is not restrictive to simplified boundary conditions, and is quite tractable given the widespread availability of inexpensive high-speed computing power. Indeed, we take this approach in our work to produce theoretical DLVO force curves that are valid over a wide range of salt concentrations, surface potentials, and separations. We use the powerful method of Galerkin finite element analysis⁴⁶ to obtain a numerical representation of the governing potential distribution.

Care must be taken when comparing DLVO predictions to direct force measurements between dissimilar surfaces. In particular, decoupling the potential of one surface from the other when fitting the data to theoretical predictions becomes an almost impossible task; hence, meaningful application of theory requires knowledge of one of the two substrate boundary conditions. One can, for example, derive this information from an independent set of force measurements (involving just one of the two substrates). We follow this strategy in comparing DLVO predictions

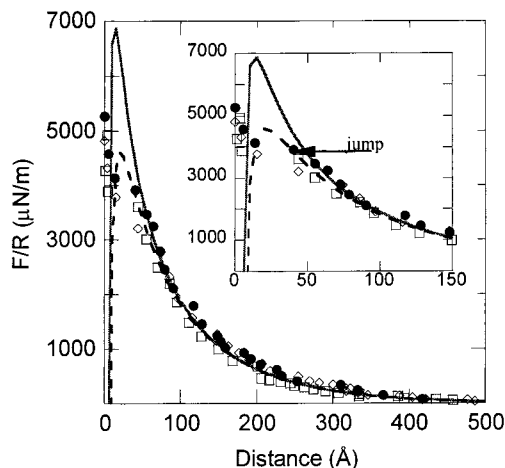


Figure 1. Measured forces (normalized with the radius of curvature) between two mica surfaces in 10^{-3} M KClO_4 . The inset shows force at short separation. The lines correspond to the best fit DLVO prediction for a Debye length of 96 nm and at -107 mV. The upper line is for constant charge and the lower (dashed) line is for constant potential.

between potential-controlled gold and mica as presented later in this paper. It is interesting to briefly discuss these experiments here, however, as they serve to confirm the validity of DLVO theory as well as to establish the variability of mica surface properties.

Previous investigations have revealed that the surface potential of mica varies with composition,⁸ i.e., from one sample to another. Hence, mica used in any one of our gold–mica experiments was always one of a set obtained from the same larger freshly cleaved mica piece. The others from the set were employed in an independent mica–mica force experiment performed at the same salt concentration. DLVO theory was then used to determine the surface potential or surface charge density of the mica by fitting predictions to the measured mica–mica force curve. For the particular gold–mica experiment presented in this paper, we obtained a value of surface potential for the mica of 107 ± 10 mV, similar to that obtained in other force experiments reported in the literature.^{8,10–14} The force curves as well as the best theoretical fits are shown in Figure 1. We note that we saw a jump into contact at a concentration of 1 mM, which was not observed by Pashley and Israelachvili^{10,11} but was observed by Shubin and Kekicheff.⁴⁷ We also examined the variation of mica surface potential when we used mica from four different mica sheets (all different pieces of ruby mica); notably, the surface potential is fairly constant across the series: 110 ± 14 mV. Hence, it appears that the variations arising from different mica sheets are not significantly greater than random error within a single experiment.

Electrochemical Surface Forces Apparatus

The chief hurdle in turning an SFA into an ESFA is development of electrode substrates that do not limit the basic functionality of the apparatus. The classic substrates employed in the conventional SFA are molecularly smooth mica sheets, approximately 1 cm^2 in area. To allow the application of MBI, these transparent substrates ($3\text{--}7 \mu\text{m}$ in thickness) are coated with silver on one of their sides and loaded into the apparatus so as to form a high-fidelity Fabry–Perot interference filter (of the configuration silver/mica/intervening medium/mica/silver).

(47) Shubin, V. E.; Kekicheff, P. *J. Colloid Interface Sci.* **1993**, *155*, 108–123.

(39) Gouy, G. *J. Phys. Radium* **1910**, *9*, 457–468.

(40) Chapman, D. L. *Philos. Mag.* **1913**, *25*, 475–481.

(41) Ninham, B. W.; Parsegian, V. A. *J. Theor. Biol.* **1971**, *31*, 405 ff.

(42) Chan, D. Y. C.; Mitchell, D. J. *J. Colloid Interface Sci.* **1983**, *95*, 193–197.

(43) Bell, G. M.; Peterson, G. C. *J. Colloid Interface Sci.* **1972**, *41*, 542–566.

(44) Hunter, R. J. In *Modern Aspects of Electrochemistry*; Plenum Press: New York, 1975; Vol. 11, pp 33–84.

(45) Russel, W. B.; Saville, D. A.; Schowalter, W. R. *Colloidal Dispersions*; Cambridge University Press: New York, 1989.

(46) Strang, G.; Fix, G. *An Analysis of the Finite Element Method*; Prentice Hall: Englewood Cliffs, NJ, 1973.

In the ESFA, we substitute a gold electrode for one of the mica substrates, while maintaining the fundamental capabilities of the SFA. Although we have previously shown how metal films can be effectively utilized in the SFA, the development of an ESFA requires the nontrivial step of turning these films into functional electrodes.

The most demanding requirement in the electrode preparation is to attach a wire to the metal surface without affecting the interferometry or contaminating the surface. We accomplish this by adapting a wire attachment technique that was previously developed in the Vanderlick laboratory.⁴⁸ In short, the success of this technique rests on the use of a mask (made of mica) to create an inhomogeneous gold film: the central region, which is implicated in the force measurements, is optimized for application of MBI; a thicker more robust peripheral region allows efficient attachment of the wire.

The exact electrode preparation process is as follows: a clean molecularly smooth piece of mica is glued to the standard silica support disk employed in the SFA. The center of this mica piece is then masked by another, smaller piece of mica, which is held in place by van der Waals forces. Masking the glued mica sheet protects the central region from the surroundings during the upcoming soldering process. Next, an adhesive layer of chromium (ca. 10 nm) is evaporated on the mica followed by a thick layer (ca. 150 nm) of gold. The result is a robust adherent film suitable for wire attachment. Pure indium is then used to solder a fine gold wire to the gold-covered mica sheet; the wire is attached beyond the area of the underlying mask. Indium alloys well with gold and yields a strong bond. It is important to note that no flux or surface treatment is necessary to solder the wire. Next, the connection is covered with epoxy; this important step in the process is necessary to prevent corrosion during utilization in an electrochemical environment. Last, the smaller piece of mica is removed with tweezers (revealing a bare patch of mica) and the disk is put in the evaporator to deposit a final gold layer that is thin enough for interferometry (ca. 65 nm). (Note that a fresh gold layer now completely covers the entire substrate.) The electrode is used in the SFA immediately after the final evaporation. It should be stressed that the gold surface used in force measurements is polycrystalline and that double layer characteristics are dependent on crystal orientation.^{49,50}

Beyond electrode preparation as described above, potential control in the force apparatus requires few additional considerations. We use a Teflon bath for the electrolyte instead of filling the whole chamber. Using the bath provides extra room inside the chamber to install wires and avoids galvanic corrosion. The gold electrode described previously is connected to a potentiostat as a working electrode. A gold wire is used as a quasi-reference electrode,⁵¹ and gold gauze is used as the counter electrode. This arrangement allows us to use the gold surface in a three-electrode cell arrangement inside the SFA. In other words, the potential of the gold surface is measured with respect to the reference electrode while the required current flow needed to control potential is passed between the counter and the working electrode.⁵²

(48) Knarr, R. Ph.D. Thesis, Chemical Engineering, University of Pennsylvania, 1999.

(49) Hamelin, A. *J. Electroanal. Chem.* **1996**, *407*, 1–11.

(50) Hamelin, A.; Vitanov, T.; Sevastyanov, E.; Popov, A. *J. Electroanal. Chem.* **1983**, *145*, 225–264.

(51) Fisher, D. J.; Belew, W. L.; Kelley, M. T. In *International Congress of Polarography*; Hills, G. J., Ed.; Interscience Publisher: 1966; Southampton, 1964; Vol. 2, pp 1043–1058.

(52) Bard, A.; Faulkner, L. R. *Electrochemical Methods Fundamentals and Applications*; John Wiley & Sons: New York, 1980.

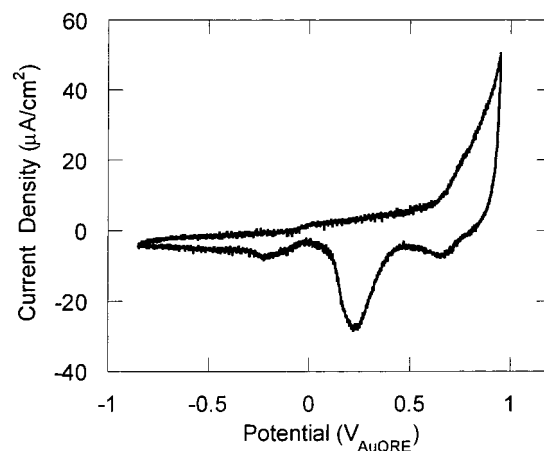


Figure 2. Cyclic voltammogram obtained in the SFA. Potential is measured with respect to a gold quasi-reference electrode. The salt concentration is 10^{-3} M KClO_4 , and the scan rate is 25 mV/s.

The potential window in which electrode charging is capacitive is the double layer region and can be determined by cyclic voltammetry. Figure 2 shows a cyclic voltammogram produced in the ESFA not only confirming the functionality of the electrode but also establishing that double layer charging will be the main cause of surface forces between -0.8 and 0.5 V_{AuQRE} . The voltammogram produced in the ESFA shows the general characteristics of a polycrystalline gold electrode but is not as well-defined as those obtained in carefully controlled electroanalytical experiments.⁵³ After the force measurements, the potential of the quasi-reference electrode was measured to be -0.310 V vs Ag/AgCl.

In designing and interpreting force measurements employing an electrode, it is important to distinguish between the electrode potential and the surface potential.⁵⁴ The electrode potential is measured with respect to a reference electrode while the surface potential is the potential used in the Poisson–Boltzmann equation assuming that the solution potential is zero. DLVO theory gives the surface potential while the potentiostat controls the electrode potential. Although the electrode potential controls the surface potential, there is no direct relationship between the two.

The remaining important point that must be addressed in utilizing the electrode in force measurements is the impact of roughness on the application of MBI. We have previously addressed the issue in detail,^{55,56} and the salient points will be summarized here. In the case of an experiment involving interactions between a metal electrode and mica, a viable interference filter is created by coating the backside of the mica sheet with a silver coating, as is done in a conventional SFA experiment. In this case, however, the resulting optical filter (comprised of gold/solution/mica/silver) is unsymmetrical and harbors internal roughness (as associated with the gold surface).

The unsymmetrical nature of the optical filter obviates the use of simplified analytical expressions for accurate measurement of surface separation as determined from fringe wavelength information. Instead, the multilayer

(53) Clavilier, J.; Nguyen Van Huong, C. *J. Electroanal. Chem.* **1977**, *80*, 101–114.

(54) Bockris, J. O. M.; Khan, S. U. M. *Surface Electrochemistry: A Molecular Level Approach*; Plenum Press: New York, 1993.

(55) Levins, J. M.; Vanderlick, T. K. *J. Colloid Interface Sci.* **1997**, *185*, 449–458.

(56) Levins, J. M.; Vanderlick, T. K. *J. Colloid Interface Sci.* **1993**, *158*, 223–227.

matrix method must be employed, which requires explicit knowledge of substrate thicknesses. In practice, this means that the mica thickness must be determined in an independent experiment (e.g., contact fringes must be measured in a separate mica–mica experiment using mica of equivalent thickness to that employed in the ESFA).

Meanwhile, accurate determination of the separation between the gold and the mica substrates, as deduced from observed fringe wavelengths, must take into account the roughness of the gold surface. We have previously shown that contact between rough gold and mica can be effectively modeled as a smooth gold film separated from mica by a thin layer of dielectric material (of thickness on the order of the root mean square surface roughness).⁵⁵ The thickness of this “residual” dielectric can be determined by comparing the positions of observed contact fringes to those obtained in the absence of surface roughness. In doing so, we obtained for our gold electrode an effective residual dielectric thickness of $44 \pm 3 \text{ \AA}$, which is very similar to the value of 47 ± 4 and $44 \pm 4 \text{ \AA}$ observed by Levins and Vanderlick for gold films previously fabricated in our laboratory. In a force experiment, wherein the electrode and mica are separated from contact, the separation is deduced by determining the increase in dielectric thickness (beyond the “residual” thickness) needed to predict the observed interference fringes. Finally, we note that contact between gold and mica, especially under high loads (on the order of 10 mN) induces measurable changes in degree of roughness.⁵⁷ In our experiments, we took care to limit the total load applied (to under 0.1 mN) and so we did not take into account change in roughness.

Last, it is possible to employ two metal electrodes in the SFA; however, certain complications must be addressed. One of the most significant is that the metal films must be very thin so as to avoid a black out region corresponding to severely diminished fringe intensities occurring when the surfaces are close to contact;^{15,58} at the same time, very thin films have a high electric resistance and might also inhibit proper potential control. Cold welding between two metal surfaces may also occur.⁵⁹

Experimental Section

Materials. Solutions of $1 \times 10^{-3} \text{ M}$ of KClO_4 were prepared from the highest available purity (99.99+%, Aldrich, Milwaukee, WI) and used without further purification in 18.2 M Ω deionized water (Hydro Services and Supplies, Levittown, PA). The solution was unbuffered and had a pH of approximately 5.5. The gold working electrode was prepared by thermal evaporation at a rate of 2.0–2.5 $\text{\AA}/\text{s}$ using high-purity gold (99.999%, Cerac, Milwaukee, WI). The characterization of the roughness of the evaporated sample was described elsewhere^{55,59} as having an average roughness of 2 nm. A piece of gold wire (99.95%, Alfa, Ward Hill, MA) was used as a quasi-reference electrode, and a 1 cm² gold gauze (82 mesh, 99.9%, Alfa, Ward Hill, MA) was used as counter electrode. Solder was high-purity indium (99.99%, Cerac, Milwaukee, WI) and covered with epoxy (Hysol 0151, Dexter, Bay Point, CA). Mica sheets (Ruby, ASTM V-2, S&J Trading, Glenn Oaks, NY) were cleaved in a laminar hood and put on a larger mica backing sheet. Silver (99.999%, Alfa, Ward Hill, MA) was evaporated on the backside at 3.5 $\text{\AA}/\text{s}$. Mica was glued silver side down on a silica disk with epoxy (Shell Epon 1004).

Cleaning. All stainless steel parts that come into contact with electrolyte (spring, upper, and lower disk holder) were cleaned in an RBS (Pierce, Rockford, IL) detergent solution, passivated

in 50% nitric acid solution, rinsed thoroughly with ethanol, and dried immediately before use. All of the Teflon parts (bath, tubing assembly) were cleaned in a detergent solution, rinsed thoroughly with water, and dried with nitrogen immediately before use. All glassware was cleaned with detergent, rinsed with water, soaked in 50% sulfuric acid solution, and rinsed thoroughly with hot water. Gold counter and reference electrodes were cleaned with piranha solution (3:7 $\text{H}_2\text{O}_2:\text{H}_2\text{SO}_4$), rinsed, and dried with nitrogen before the experiment.

Procedure. Once the apparatus was completely assembled with all electrical connections in place, gold and mica were brought into contact in air and the fringe positions were recorded. The surfaces were then separated, and the solution was injected using a reagent bottle equipped with all Teflon tubing and valves (Omnifit, Rockville Center, NY) pressurized with humid nitrogen. The solution was deaerated with humid nitrogen for 30 min before use, and the experiment was done under a slight positive pressure of humid nitrogen. The solution was left in the apparatus for 1–2 h for equilibration. Then, cyclic voltammograms were performed in the SFA to establish the double layer region. The potential was controlled and the current monitored with a potentiostat (EG&G 263A, Perkin-Elmer, Oakridge, TN). Surface forces were measured at a potential set by the potentiostat. For each potential, forces were repeated at least once. The potentiostat was also monitoring current during the force measurements to ensure that there was no faradaic current. At the end of the experiment, the radius of curvature was measured using a CCD camera (Photometrics, Tucson, AZ). For experiments involving two mica surfaces, the same procedure was followed without the use of electrodes. All experiments were performed at 22 $^\circ\text{C}$.

Results and Discussion

The new ESFA was used to measure forces between a gold electrode and molecularly smooth mica. We chose to study forces in KClO_4 solution because it has been established that perchlorate ions do not specifically adsorb on gold.⁵⁰ Shown in Figure 3 are measured force curves at different applied potentials. As is readily seen, by changing potential, we are to modulate, in situ, without change of surface or solution, the character of forces from attractive to very repulsive. Forces were quite reproducible at all applied potentials, as illustrated by the multiple force runs shown in Figure 3. It is worth noting that force curves are taken over a much larger time period with the ESFA than with an AFM. This means that the applied surface potential is stable over a long period of time (minutes).

Also shown in Figure 3 are predictions from DLVO theory. We used a Hamaker constant of $8.4 \times 10^{-20} \text{ J}$ to model the van der Waals interaction between gold and mica. This value corresponds to the geometric average between the published Hamaker constant for gold²³ ($(25-40) \times 10^{-20} \text{ J}$) and the mica⁸ ($2.2 \times 10^{-20} \text{ J}$). As previously described (see Figure 1), the mica surface characteristics are established in an independent experiment.

In general, as is readily seen, the theoretical predictions correspond well to the measured forces at long range, but at separations below ca. 50 \AA , significant deviations are observed. At applied potentials between -0.3 and -0.2 V (Figure 3d–f), forces are small and surfaces jump into adhesive contact. Here, the choice of Hamaker constant has a significant impact on the theoretical predictions and more accurate values may give even better fits. As potential is increased between -0.4 and -0.7 V (Figure 3a–c), deviations from theory become more apparent, with strong repulsive forces observed at short range; similar non-DLVO forces have often been observed in many other force measurements (note that the origin of short range double layer forces is a matter of debate; see, for example, the work of Shubin and Kekicheff⁴⁷). Although adhesive contact is established at low potentials, contact at high potentials is purely repulsive.

(57) Quon, R. A.; Knarr, R. F.; Vanderlick, T. K. *J. Phys. Chem. B* **1999**, *103*, 5320–5327.

(58) Clarkson, M. T. *J. Phys. D: Appl. Phys.* **1989**, *22*, 475–482.

(59) Knarr, R.; Quon, R. A.; Vanderlick, T. K. *Langmuir* **1998**, *14*, 6414–6418.

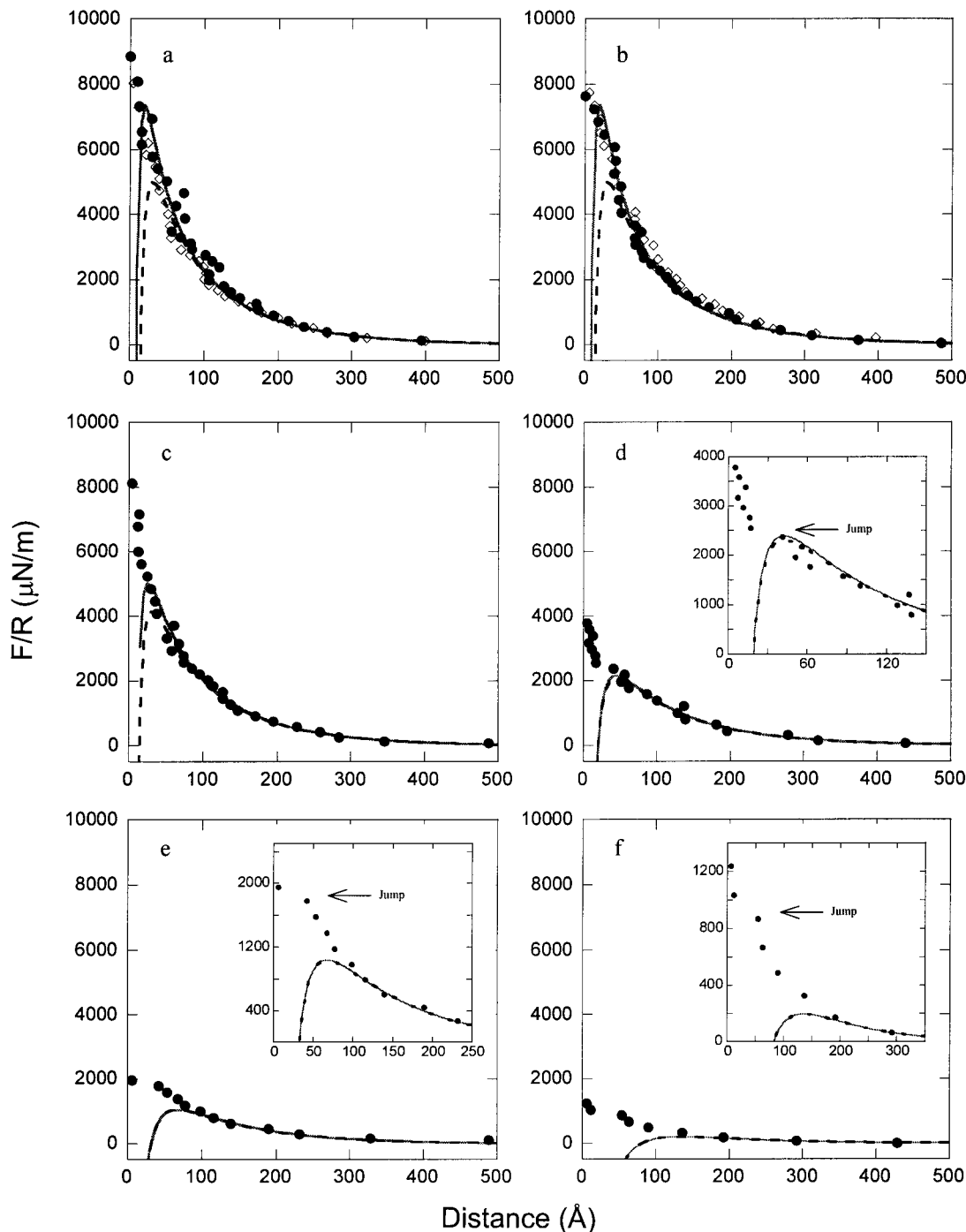


Figure 3. Measured and theoretical forces (normalized with the radius of curvature) between gold and mica. The gold surface is under potential control, with respect to a gold quasi-reference electrode at (a) -700 mV, DLVO fit at -185 mV; (b) -600 mV, DLVO fit at -185 mV; (c) -400 mV, DLVO fit at -115 mV; (d) -300 mV, DLVO fit at -85 mV; (e) -250 mV, DLVO fit at -60 mV; and (f) -200 mV, DLVO fit at -25 mV. Insets represent an enlargement of forces at short separation. In all cases, the Debye length was set at 96 nm and the Hamaker constant was 8.4×10^{-20} J. In the theoretical fit, gold was set at constant potential. Upper lines correspond to mica at constant charge and lower (dashed) lines correspond to mica at constant potential. The mica potential was -107 mV as determined in a previous experiment (see Figure 1).

While the force data itself is quite reproducible, we note that the sensitivity of fitting it to DLVO theory is severely diminished as potential is increased (in other words, at higher applied electrochemical potentials, marked variations in surface potential result in little change in predicted force curves). This phenomenon is, in fact, a ramification of the saturation effect, as described later.

The range of surface potentials we achieve in our ESFA is particularly notable: a spread of almost 200 mV, shown in Figure 3. Hillier et al.²³ studied interactions over a wide applied potential range but did not observe a

corresponding large variation in surface potentials (as fitted from DLVO theory). Raiteri et al.²⁴ observed a wide range of forces but could not compare directly with DLVO theory because of uncertainties in tip geometry.

DLVO theory predicts that forces of interaction saturate (i.e., reach a maximum) as potential are increased as shown in Figure 4. Our experiments confirm this behavior (see Figure 3). The onset of saturation can be conveniently established by plotting, as a function of surface potential, the force evaluated when the surfaces are 7.5 nm apart; at this distance, interactions are governed primarily by

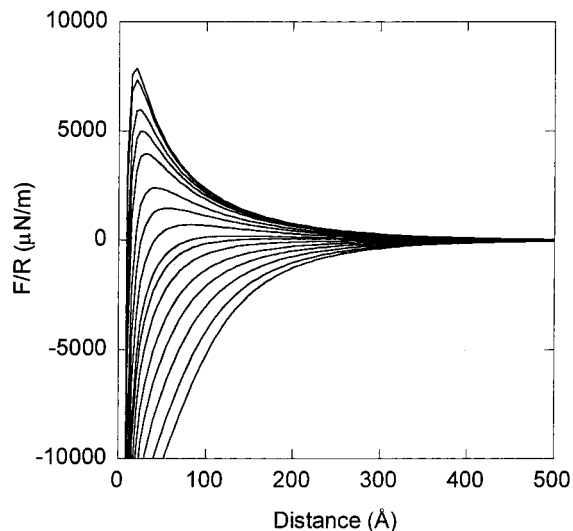


Figure 4. Theoretical prediction of surface forces (normalized with the radius of curvature) between gold and mica in 10^{-3} M aqueous solution. Mica is set at constant charge with a corresponding surface potential of -107 mV as determined previously (see Figure 1). Forces curves are calculated for different values of gold surface potential. As gold potential is made more negative, the change in forces reduces and tends to saturate. The values of gold potentials for calculations were (from the top to bottom, in mV) -200 , -185 , -155 , -135 , -115 , -85 , -65 , -45 , -25 , -15 , 0 , 20 , 40 , 65 , 100 , and 150 .

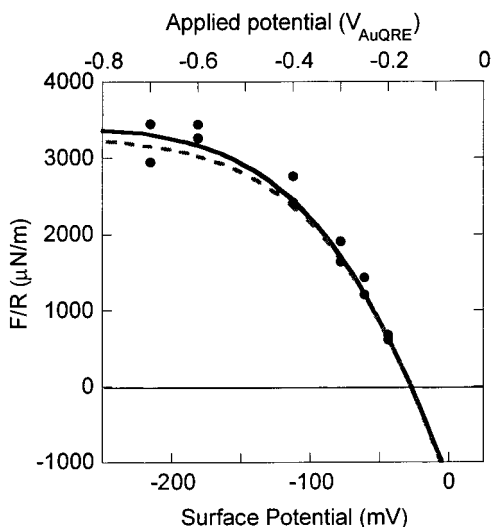


Figure 5. Onset of saturation. Measured value of forces at a separation of 75 nm (data). Corresponding DLVO forces at 75 nm for different gold surface potential. The continuous line corresponds to mica at constant charge, and the dashed line corresponds to mica at constant potential (dashed) at a value of 107 mV and a Debye length of 96 nm. Experimental data were scaled linearly on the potential axis to match the surface potential.

electrostatic interactions (in relation to van der Waals and/or short range forces). The result, shown in Figure 5, reveals that the saturation effect occurs over a narrow potential window. This finding is similar to that of Raiteri et al.²⁴ who using AFM, also observed the force saturation effect over a very narrow applied potential range. On the other hand, Hillier et al.,²³ who did similar experiments with an AFM, did not observe a saturation in forces at all.

At the other limit of low applied potentials, more positive than $-0.2 V_{\text{AuQRE}}$, interactions between the gold electrode and the mica rapidly become attractive. As a result of the mechanical instability associated with spring-based force

measurements, the surfaces jump into contact from significant separations, thus precluding detailed characterization of the entire force curve. We note that use of a stiffer spring in our apparatus could ultimately be used to characterize more fully these attractive forces. On the other hand, a stiffer spring would, however, reduce accuracy in the measurement of repulsive forces.

Surface roughness is not taken into account in traditional DLVO theory even though most surfaces and colloid particles, including our electrode, harbor a certain degree of roughness. As described in a recent review by Walz,⁶⁰ divergence between DLVO theory and experiments involving rough particles is often explained by surface roughness. Many researchers have tried to incorporate surface heterogeneity in electrostatic or van der Waals interactions.^{61–66} We do not attempt to address the effect of roughness on the modulation of DLVO forces in this paper, although we note that this is a tractable problem and one currently under investigation in our laboratory.

We note, however, that the presence of roughness appears not to preclude the general agreement between measured forces and conventional DLVO theory. In essence, our experiment is a test of the applicability of DLVO theory to rough surfaces. On the other hand, because the surface potential is a fitted parameter, the effect of roughness could present itself in the corresponding value of surface potential. It is also possible that roughness-induced deviations from DLVO theory may be small at the low salt concentrations we employ (1 mM); such deviations are predicted to increase significantly with increased salt concentration.⁶⁴

Last, we note a most interesting feature of potential control, namely, in situ control of adhesion. As discussed previously, the nature of contact observed varies from repulsive at high applied potentials to attractive at low potentials. Retraction of surfaces from adhesive contact is accompanied with jump out to large separations (on account of the inherent spring instability). The magnitude of this jump out can, in fact, be used to quantify the contact adhesion force. Indeed, we are currently undertaking experiments to elucidate the variation in adhesion with applied potential. The effect of applied potential on adhesion has been studied with AFM by Serafin and Gerwith,⁶⁷ Serafin et al.,⁶⁸ and Campbell and Hillier²⁹ and will be discussed in a subsequent paper. Meanwhile, however, from a practical point of view, adhesive contact can be an aggravating complication in surface forces experiments. In particular, the resulting jump apart jets the surfaces to an unknown separation, whereupon one must reidentify the visible fringes. Hence, the ability to control in the SFA the nature of adhesion of surfaces in contact has both practical and scientific merit.

Conclusions

In this paper, we showed how the SFA can be used to measure forces under potential control. Evaporated gold

(60) Walz, J. Y. *Adv. Colloid Interface Sci.* **1998**, *74*, 119–168.

(61) Kostoglou, M.; Karabelas, J. *J. Colloid Interface Sci.* **1995**, *171*, 187–199.

(62) Shulepov, S. Y.; Frens, G. *J. Colloid Interface Sci.* **1995**, *170*, 44–49.

(63) Suresh, L.; Waltz, J. W. *J. Colloid Interface Sci.* **1996**, *183*, 199–213.

(64) Bhattacharjee, S.; Ko, C. H.; Elimelech, M. *Langmuir* **1998**, *14*, 3365–3375.

(65) Sun, N.; Walz, J. Y. *J. Colloid Interface Sci.* **2001**, *234*, 90–105.

(66) Bhattacharjee, S.; Elimelech, M. *J. Colloid Interface Sci.* **1997**, *193*, 273–285.

(67) Serafin, J. M.; Gewirth, A. A. *J. Phys. Chem. B* **1997**, *101*, 10833–10838.

(68) Serafin, J. M.; Hsieh, S.-J.; Monahan, J.; Gewirth, A. A. *J. Phys. Chem. B* **1998**, *102*, 10027–10033.

on mica was employed as an electrode set in a three-electrode configuration. We used a masking technique to produce electrodes that are suitable for electrochemistry as well as interferometric measurements. The method presented is not restricted to gold. Other highly reflective metals such as silver and platinum could also be used in this arrangement.

We applied the technique to investigate double layer forces at different applied potential. We observed a notable variation in surface forces as a function of applied potential ranging from attractive to highly repulsive. The long range forces correspond well to DLVO prediction, including evidence of saturation in forces at high applied potentials, and there is deviation in forces for short range interactions.

This technique could be used to study a wide variety of surface phenomenon such as potential-controlled adhesion; potential dependent adsorption; the effect of rough-

ness on surface forces, and the effect of potential on roughness. Indeed, it is known that cyclic voltammetry roughens electrode surfaces.^{69,70} The availability of smooth electrode surfaces has particular value for all of these studies. As we have previously demonstrated,⁵⁹ such surfaces can be fabricated in the SFA using a procedure based on cold welding.

Acknowledgment. We gratefully acknowledge the National Science Foundation (CTS-9907687) for support of this work.

LA011087K

(69) Robinson, K. M.; Robinson, I. K.; O'Grady, W. E. *Electrochim. Acta* **1992**, *37*, 2169–2172.

(70) Strbac, S.; Hamelin, A.; Adzic, R. R. *J. Electroanal. Chem.* **1993**, *362*, 47–53.